

Skin-color-independent robust assessment of capillary refill time

Raquel P. de Souza Bachour¹, Eduardo Lopes Dias¹, and George C. Cardoso¹

¹Universidade de Sao Paulo Campus de Ribeirao Preto

August 17, 2023

Abstract

Capillary Refill Time (CRT) assesses peripheral perfusion in resource-limited settings. However, the repeatability and reproducibility of CRT measurements are limited for individuals with darker skin. This paper presents quantitative CRT measurements demonstrating good performance and repeatability across all Fitzpatrick skin phototypes. The study involved 22 volunteers and utilized controlled compression at 7 kPa, an RGB video camera, and cocircular polarized white LED light. CRT was determined by calculating the time constant of an exponential regression applied to the mean pixel intensity of the green (G) channel. An adaptive algorithm identifies the optimal regression region for noise reduction, and flags inappropriate readings. The results indicate that 80% of the CRT readings fell within a 20% range of the expected CRT value. The repetition standard deviation was 17%. These findings suggest the potential for developing reliable and reproducible quantitative CRT methods for robust measurements in patient triage, monitoring, and telehealth applications.

Skin-color-independent robust assessment of capillary refill time

Raquel P. de Souza Bachour; Eduardo Lopes Dias; George C. Cardoso

¹Department of Physics, FFCLRP,
University of Sao Paulo, 14040-901, Brazil

Abstract. *Capillary Refill Time (CRT) assesses peripheral perfusion in resource-limited settings. However, the repeatability and reproducibility of CRT measurements are limited for individuals with darker skin. This paper presents quantitative CRT measurements demonstrating good performance and repeatability across all Fitzpatrick skin phototypes. The study involved 22 volunteers and utilized controlled compression at 7 kPa, an RGB video camera, and circular polarized white LED light. CRT was determined by calculating the time constant of an exponential regression applied to the mean pixel intensity of the green (G) channel. An adaptive algorithm identifies the optimal regression region for noise reduction, and flags inappropriate readings. The results indicate that 80% of the CRT readings fell within a 20% range of the expected CRT value. The repetition standard deviation was 17%. These findings suggest the potential for developing reliable and reproducible quantitative CRT methods for robust measurements in patient triage, monitoring, and telehealth applications.*

Keywords— Capillary refill time, Peripheral perfusion, non-invasive monitoring

1. Highlights

- The method is robust, presenting similar performance and good repeatability for all Fitzpatrick phototypes.
- The proposed method automatically flags most outliers and inadequate measurements.
- The method uses low compression (7 kPa), benefiting people with sensitive skin.

2. Introduction

Capillary refill time (CRT) is one of the most widely acknowledged and used methods [1, 2] to estimate peripheral perfusion status [3, 4, 5], for quick assessment or in low-resource environments. CRT is defined as the time it takes for a distal capillary bed to regain its normal color after having received enough mechanical compression to cause blanching [6, 7] of the skin surface. Compression is typically applied by the finger of the person who measures, who uses a chronometer and their own visual assessment to measure the refill time [8, 9, 10]. CRT measurements sites in humans include the sternum [11], on the forearm [12], in the legs and feet [10, 13, 14], in the fingertips [15, 16], and the knees [17, 18]. When performed in ideal conditions by trained professionals, CRT has been used to diagnose septic shock [19], dehydration in children [3, 20, 21], and viral diseases, such as dengue [22], and, more recently, as a prognostic factor in patients with COVID-19 [23].

39 Among CRT's main advantages are simple equipment, high speed, and simplicity
40 in training. Yet, the adoption of CRT is hampered by concerns about its inter- and intraob-
41 server reproducibility, a lack of standardization for pressure and duration of compression
42 [4, 7, 24, 25], the effect of external factors such as the lighting in the room [26] and the
43 temperature of the limb and the environment [7, 13, 27], and the effect of skin color, par-
44 ticularly dark skin, on CRT accuracy [6, 18, 28]. These limitations have called into ques-
45 tion the applicability and usefulness of manual CRT measurements [7, 19, 29]. Attempts
46 to improve the reliability and objectivity of CRT measurements include the proposal of a
47 device that utilizes optical assessment of diffuse reflectance on the skin to calculate the
48 CRT [12], a device comprising a compressible plastic optical fiber to measure CRT under
49 the foot [14], and a video camera system for training personnel to perform traditional CRT
50 measurements [30].

51 Video-based CRT measurements [24, 31, 32, 33, 34] have been proposed due to
52 the higher sensitivity and linearity of RGB cameras compared to the human eye. Cameras
53 allow for the detection of subtle hues and intensity changes between the time of skin
54 compression and its capillary refilling to the original state. While some studies simply
55 visually analyze the CRT videos at a later time [34], others automate video processing
56 [32]. Shinozaki et al. [24] acquire the RGB channels' intensities during a fingertip test, fit
57 an exponential decay between the instants of maximum compression and of 90% recovery
58 and obtain CRT with success. We could not find studies in the literature addressing issues
59 such as CRT uncertainties, reproducibility, reliability, and robustness with respect to skin
60 phototypes. In addition, the literature lacks studies of CRT under controlled conditions.

61 In the present paper, we show that CRT can be made robust and reliable, at least
62 by using controlled compression, video processing, and polarized light. By robust, we
63 mean insensitive to perturbations such as measurement repetitions and measurement re-
64 productions with changes in skin phototypes. By reliable, we mean that inadequate or
65 poor measurements are identified and flagged to be repeated. Our method is based on
66 recording a video of a region of interest (ROI) after the release of the compression. It uses
67 image processing and curve fitting to calculate the CRT, and cocircular polarizers between
68 the light source and the camera to attenuate the light reflected on the outer surface of the
69 skin. We tested our method on 22 volunteers, including all Fitzpatrick phototypes, under
70 controlled conditions of temperature, lighting, and applied pressure.

71 To distinguish our CRT method from other studies in the literature, we name it
72 *polarized CRT* (*pCRT*). The polarized light is not essential but is known to increase ro-
73 bustness in skin measurements. This terminology will be adopted for the remainder of the
74 paper.

75 **3. Materials and methods**

76 **3.1. Study subjects**

77 We chose to invite volunteers that represented all Fitzpatrick skin types, and aged above
78 20 years. Twenty-two healthy volunteers (aged 20 to 70 years; 9 female), comprising
79 all Fitzpatrick skin types (I-II; III-IV, and V-VI) chose to participate in this study after
80 being detailed about the procedure (University of São Paulo Ethics Committee CAAE
81 95342518.1.0000.5407, 3.046.098 FFCLRP).

82 3.2. Experimental protocol

83 We have built a cylindrical compression device to produce skin blanching on the volun-
84 teer's forearm (Figure 1(a)). The cylindrical device (Aluminum) smoothly slid inside a
85 hollow external acrylic cylindrical vest to gently rest on the volunteer's forearm. To ther-
86 mally insulate the metallic cylinder from the skin, it was capped with a circular Teflon cap
87 (4 cm^2) featuring rounded corners. The rounded corners' radius were sufficient to prevent
88 pressure marks in the skin.

89 An LED light source (E27, TKL-90 model, 14 W, Taschibra Ltda, Brazil) was used
90 to illuminate the forearm. As a precautionary measure for experimental reproducibility in
91 this study, the light source was activated at least 15 minutes prior to each data acquisition
92 to avoid potential warm-up transient effects.

93 The video camera were recorded at 30 frames per seconds (HD Pro-C525,
94 1280×720 pixels, video container: WMV, encoding: YUV12; Logitech S.A., Switzer-
95 land) and the light source were attached to a fixture (Figure 1 (b)). The camera was
96 focused on each subject's region of interest (ROI) on the forearm, 9 cm from the wrist
97 line. To block specular reflections [35, 36], cocircular detection [37] was used. Circular
98 polarizers ($\lambda/4 = 125\text{ nm}$, 99.98% polarization efficiency, crossed transmission 0.5%, 3D
99 Lens Corp., Taiwan ROC) were placed both in front of the light source and camera lens,
100 with their quarter-wave plate sides facing the forearm (P1 and P2 in Figure 1 (b)).

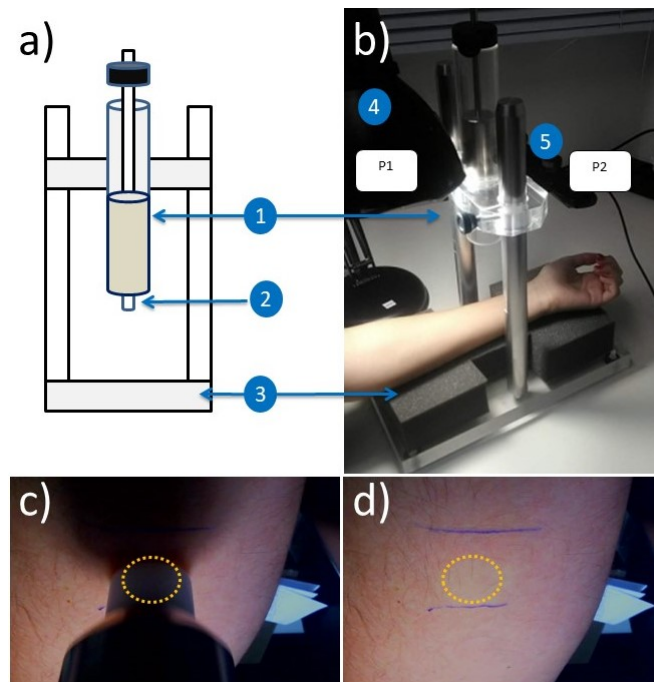


Figure 1. Experimental setup. a) Schematic illustration of the weight and arm support, front view; (1) Standard aluminum cylindrical weight; (2) thermally insulating Teflon cap (4 cm^2), that comes into contact with the subject's skin; (3) Armrest (dense polyurethane foam). b) Setup with a volunteer's arm in actual measurement position; (4) light source and (5) video camera, with cocircular polarizers (P1 and P2) installed. c) Weight lowered on a volunteer's forearm as viewed by the video acquisition camera. The ROI is highlighted by the dotted circle. d) Blanching of the ROI after the release of compression.

101 The experiments were performed in a temperature-controlled room (20°C – 22°C)
 102 as suggested by Pickard et al. [7]. All videos were acquired in a dark room illuminated
 103 only by the circularly polarized light source. Before the start of the measurements, the
 104 volunteers remained seated for 10 minutes for acclimatization. The volunteers sat in a
 105 relaxed position on a height adjustable chair with their left arm positioned approximately
 106 at the heart level (Fig. 1 (b)). For each measurement, the camera started recording the ROI
 107 for 10 s before the weight was lowered on the subject’s left forearm, where it remained for
 108 5 s applying a pressure of 7 kPa, after which it was lifted for recording the capillary refill.
 109 The recording was stopped 20 s after the lifting of the weight, which is much longer than
 110 the capillary refill times. These pCRT readings were repeated five times for each subject,
 111 with a 1-minute rest between readings. The WMV video files were processed offline at a
 112 later time.

113 3.3. Video analysis and pCRT calculation

114 The placement and subsequent removal of the cylindrical weight from the skin surface
 115 result in a pronounced color alteration. The average intensities of the R, G, and B channels
 116 of the ROI pixels are calculated for each frame (Figure 2 (a)) and the G-channel (Fig. 2
 117 (a)) presents the best signal-to-noise ratio. We hypothesized that the behavior of the G-
 118 channel decay during CRT can be modeled by an exponential decay. However, a single-
 119 exponential decay model quickly fails after a few time constants: the decay time constant
 120 changes and/or intensities become noisy (see Figure 2(a)) and Figure 3). Thus, we have
 121 devised a multistep protocol to realize the exponential regression.

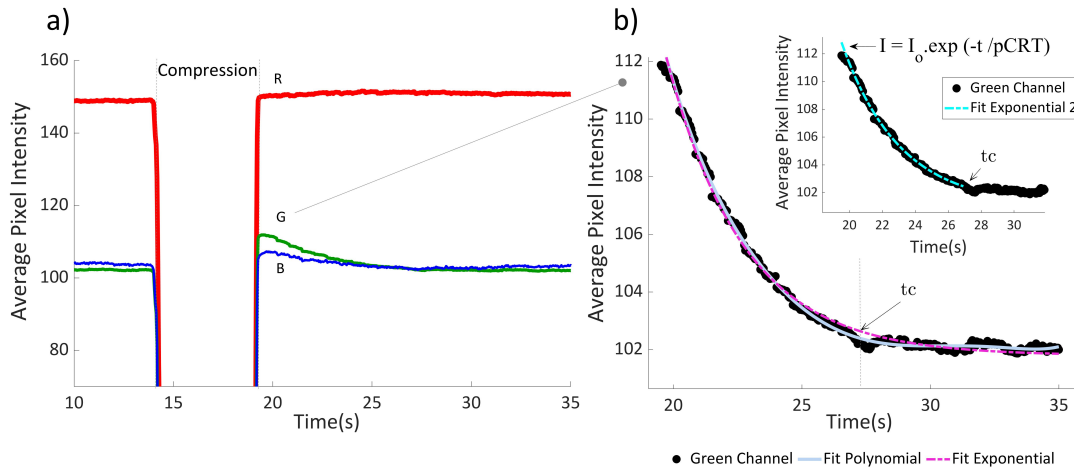


Figure 2. Mean ROI pixel intensities during a pCRT experiment (for a volunteer of phototype III-IV). a) Mean intensities of the R, G and B channels from the pixels inside the ROI. The cylindrical weight blocking the camera during compression causes the sharp drop in intensities observed between 14 s and 19 s. After the weight is lifted, the G-channel displays a pronounced peak and a decay, which is highlighted in b) Behavior of the G-channel after the compression is lifted. The decay is approximately exponential but levels off after the *cutoff time* (t_c); the inset shows the exponential regression only up to t_c , used to determine pCRT.

122 First, we identified a cutoff time t_c , after which the exponential decay model sig-
 123 nificantly diverges from the observed curve. To find t_c , we simultaneously fit a 6th-order

124 polynomial and a provisional exponential decay on the entire G channel intensity curve,
 125 after the release of the compression. The 6th-order polynomial is a compromise between
 126 accommodating up to three oscillations in the data, and still serving as a low-pass filter for
 127 the data. The point of maximum divergence between the polynomial and the provisional
 128 exponential identifies t_c (Figure 2(b)) and Figure 3(a)). This procedure proved to be ro-
 129 bust for all our instances. Finally, pCRT is the time constant of yet another exponential
 130 decay function:

$$I = I_o \exp\left(-\frac{t}{pCRT}\right) \quad (1)$$

131 fitted to the original data within the interval between the position of the maximum value of
 132 the G-channel and t_c (inset of Fig. 2(b)). A pCRT *reading* is obtained from the regression,
 133 where the 95% confidence interval (CI) is $pCRT \pm \sigma_{95\%CI}$. This uncertainty is not the
 134 pCRT uncertainty, but the uncertainty in the regression in one reading. The actual pCRT
 135 uncertainty is larger than $\sigma_{95\%CI}$ and can only be estimated by multiple readings of pCRT.
 136 In equation 1, the offsets in time and in intensity have been omitted for simplicity. Details
 137 can be found in code made available in the supplementary material online. The procedure
 138 described in this paragraph was applied to every acquired video.

139 We analyzed all 110 videos files (5 for each of the 22 volunteers) with scripts we
 140 specially developed for pCRT determination. The scripts were implemented in Matlab
 141 version 2015a (MathWorks, MA, USA).

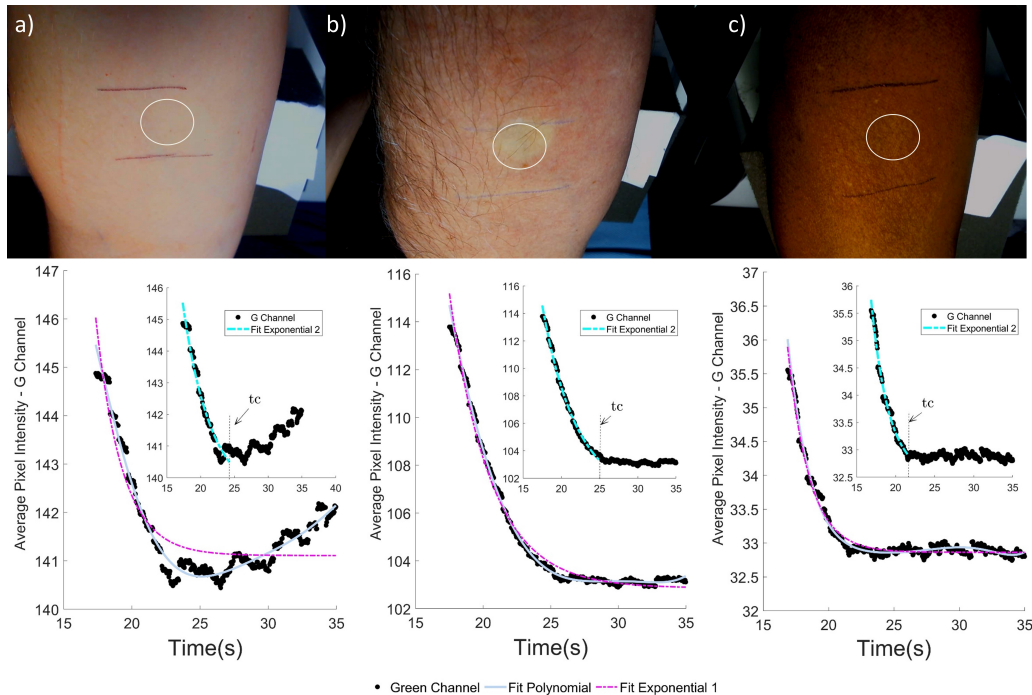


Figure 3. Forearms of different phototypes immediately after removal of the 7 kPa compression on the ROI (circle). a) Phototype I-II, b) Phototype III-IV and c) Phototype V-VI. The corresponding G-channel mean ROI intensity decay and curve regressions are shown below each volunteer image. Notice that curve behavior is not exponential for times longer than t_c .

142 3.4. Statistics and repeatability test

143 We adopted the relative uncertainty $\sigma_{95\%CI}/pCRT$, as the primary metric to assess the
144 quality of each pCRT reading. The repeatability test of pCRT was evaluated by analyzing
145 the distribution of five readings from each volunteer, from phototype groups, and for
146 all subjects together. We also established a maximum acceptable value of the relative
147 uncertainty for a single measurement, which we call the *discard-and-repeat* threshold,
148 to flag and remove readings likely to be incorrect, while keeping plausible ones. The
149 analysis of the results involved descriptive statistics to summarize the data, as well as
150 ANCOVA to account for confounding variables.

151 4. Results

152 In healthy tissue, after the skin is bleached out by compression, the color returns rapidly as
153 the blood refills the dermal capillaries. This color return is the foundation of the CRT test.
154 Our pCRT method calculates capillary refill time by analyzing the ROI's image intensity
155 over time. As shown in Figure 2, the exponential decay of intensity characteristic of
156 capillary refill is most clearly distinguishable in the G-channel. The higher signal-to-
157 noise (SNR) ratio of the G-channel held for all our measurements, across all subjects.
158 Thus, we chose to perform our analysis on the G-channel only.

159 Table 1 summarizes pCRT results for each skin phototype group. Because the age
160 distributions are different for the different phototypes, we performed an ANCOVA anal-
161 ysis to compare the average pCRT values for the different phototypes controlled for the
162 confounder age. We found the mean pCRT for the different phototypes, even after con-
163 trolled for the confounder age, do not differ significantly (p-value = 0.1528 ANCOVA).
164 We also confirmed that pCRT has a small but significant dependency on age (p-value =
165 0.0013 ANCOVA) as already reported in the literature [1, 38]. Due to the limited number
166 of volunteers (n = 22), further investigation into the relationship between CRT and age
167 is beyond the scope of our study. Our main result is that the independence of pCRT on
168 phototype suggests its robustness with respect to light absorption by the melanin.

169 Differences in the mean pCRT might stem from differences in the age groups and
170 respective standard deviations, but the small number of volunteers in each group pre-
171 vents further interpretation. Additionally, individual t-tests were conducted to compare
172 the pCRT values among the phototype groups. The results indicated no statistically signif-
173 icant differences in pCRT between Phototypes I—II and Phototypes III—IV (p = 0.815),
174 Phototypes I—II and Phototypes V—VI (p = 0.7693), or between Phototypes III—IV
175 and Phototypes V—VI (p = 0.788). These findings suggest that there is no significant
176 variation in pCRT across the different phototype groups.

177 Figure 4 show histogram of all pCRT readings. In Figure 4(a) displays pCRT
178 readings, with a mean of 3.9 s; Figure 4(b) displays the corresponding relative re-
179 gression uncertainties $\sigma_{95\%CI}/pCRT$ with a median 7.1%. One measurement, with
180 $\sigma_{95\%CI}/pCRT > 45\%$, was omitted.

181 Figure5 displays the distribution of measurement uncertainties, providing a per-
182 spective of the pCRT results for all three phototype subgroups studied. Most pCRT
183 readings exhibit a relative regression uncertainty under 10%. Note, however, a promi-
184 nent outlier with a relative regression uncertainty exceeding 45%, with a clearly incorrect

Table 1. Mean pCRT for different Fitzpatrick skin types. pCRT differences between phototype groups were not statistically significant even after accounting for age as a confounder ($p = 0.1528$, ANCOVA)

Groups	pCRT \pm SD (s)	Age \pm SD (yr.)	Number of volunteers
Phototypes I—II	4.0 \pm 0.7	27 \pm 12	8
Phototypes III—IV	4.4 \pm 1.3	46 \pm 14	9
Phototypes V—VI	3.7 \pm 1.7	44 \pm 19	5

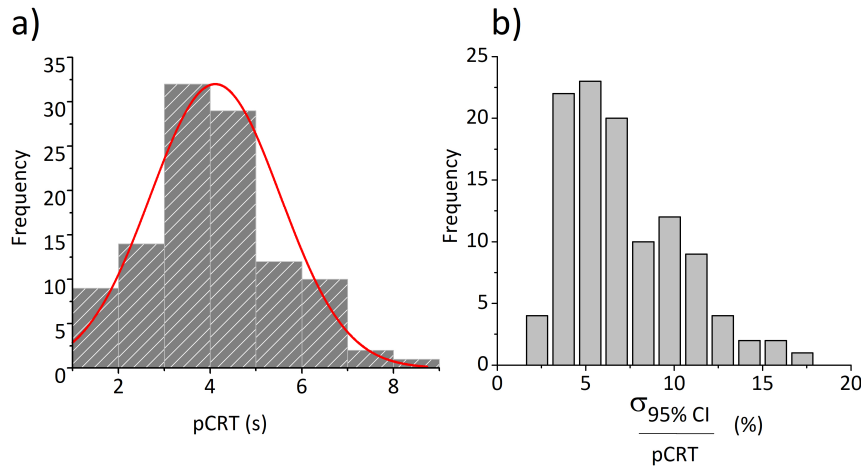


Figure 4. Descriptive statistics for all pCRT readings. a) The distribution of pCRT results for all 110 data points (5 readings for each volunteer). The red line is a Gaussian fit (mean = 3.9; SD = 1.3). b) Frequency distribution of the coefficient of variation $\sigma_{95\%CI}/pCRT$ (median = 7.1%).

185 pCRT estimate. To improve the reliability of results, we decided to flag and discard such
 186 outliers (discard-and-repeat threshold), by discarding readings with a relative regression
 187 uncertainty $\sigma_{95\%CI}/pCRT$ above 10%.

188 Figure 6 shows the results of the repeatability test. The vertical axis of Figure 6(a)
 189 represents individual pCRT readings normalized by the mean value ($\langle pCRT \rangle$) obtained
 190 from the 5 readings for each individual. The horizontal axis used box-plots to compare
 191 $\sigma_{95\%CI}/pCRT$, for the whole set (110 readings) with data with suspected outliers have
 192 been discarded by the $(\sigma_{95\%CI}/pCRT) > 10\%$ threshold (86 readings remaining). If
 193 repeatability were perfect, every reading would be identical to the average of the five
 194 readings: $pCRT/\langle pCRT \rangle = 1$ for any pCRT reading. Consequently, the relative error
 195 $\delta = |pCRT/\langle pCRT \rangle - 1|$ would be zero for all pCRT readings. However, we observe
 196 variability in the readings. For our data, $SD_{pCRT/\langle pCRT \rangle} = 30\%$ before use of the discard
 197 threshold, and $SD_{pCRT/\langle pCRT \rangle} = 17\%$ after application of the discard threshold. Thus,
 198 pCRT presents a SD of less than 20%, as the combined physiological and measurement
 199 variability.

200 Defining an acceptable reading as one that exhibits a lower than δ error relative
 201 to the average of five readings from an individual, the proportion of acceptable readings
 202 increases as the acceptable relative error δ increases (Figure 6(b)). By choosing a discard-
 203 and-repeat threshold of $\sigma_{95\%CI}/pCRT > 10\%$, approximately 80% of the original 110

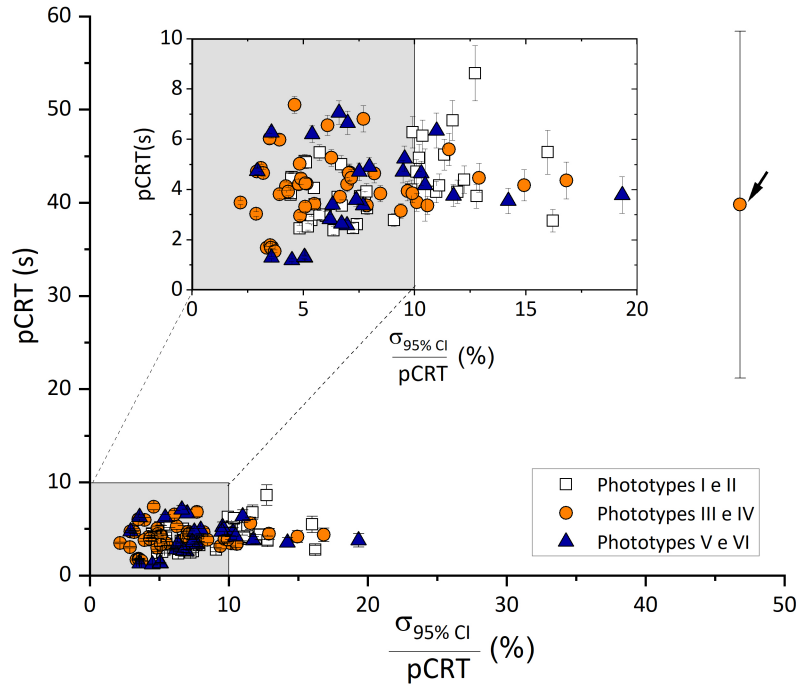


Figure 5. Distribution of pCRT readings for all phototype subgroups. All 110 readings are shown (5 for each of the 22 subjects). The error bars represent $\sigma_{95\%CI}$. The arrow highlights a point with abnormally high regression uncertainty, which indicates an erroneous measurement. The gray box in the inset shows the region with relative regression uncertainty below 10%, which is our reading's discard-threshold. Note that all phototypes are approximately equally represented and evenly distributed inside the gray box.

204 readings remained. Among these retained readings, approximately 80% fell within the
 205 range of $\langle pCRT_i \rangle \pm 20\%$, where $\langle pCRT_i \rangle$ represents the average pCRT for the i -th subject
 206 (highlighted in gray in Figure 6(b)). If precision is relaxed to $\delta > 35\%$, approximately
 207 95% of the non-discarded pCRT readings are acceptable (Figure 6(b)). The curve in
 208 Figure 6(b) is well-fitted by a logistic function ($R^2 = 0.995$), indicating that the relative
 209 error distribution remains largely Gaussian even after applying the discard threshold. A
 210 more stringent discard-and-repeat reading threshold ($\sigma_{95\%CI}/pCRT$ criterion) would flag
 211 and reject a greater number of pCRT readings. On the other hand, the proportion of
 212 acceptable readings for a given δ would increase, leading to a steeper rise of the curve
 213 illustrated in Figure 6(b).

214 5. Discussion

215 We have shown that capillary refill time can be measured repeatably and robustly, with low
 216 pressure applied to the skin. For that end, we used controlled pressure, cocircular polar-
 217 ized light imaging, and image processing. The use of cocircular polarizers[37] attenuates
 218 the reflection component of light captured by the digital camera, enabling visualization
 219 of deeper regions of the skin [39, 40]. Our system produced successful measurements
 220 in subjects with dark skin (phototypes V and VI), which are a challenge for visual CRT

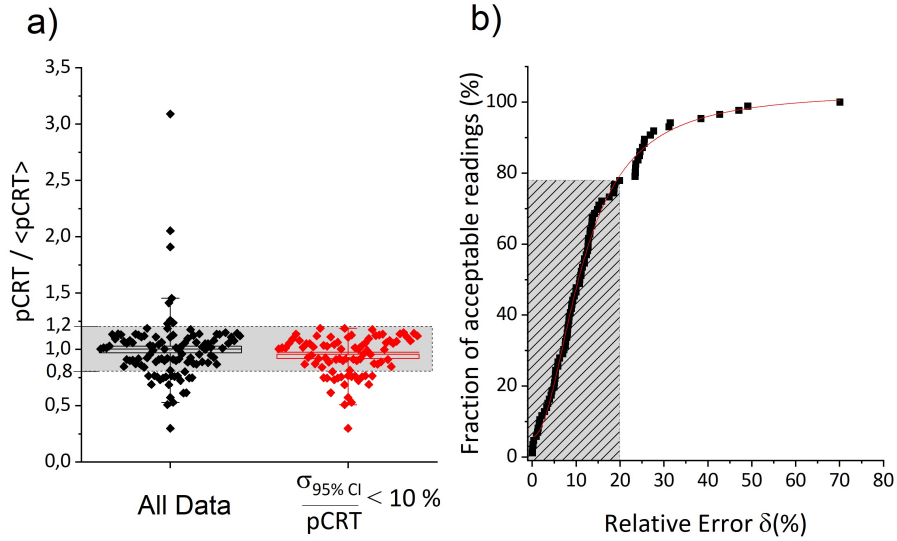


Figure 6. Repeatability analysis. a) The vertical axis represents the ratio between each pCRT reading and the mean of 5 repetitions $\langle pCRT \rangle$. The box plots compare all readings (black diamonds, 110 points, $SD_{pCRT/\langle pCRT \rangle} = 0.30$), with readings remaining after application of a 10% discard-and-repeat threshold (red diamonds, 86 points $SD_{pCRT/\langle pCRT \rangle} = 0.17$). b) Fraction of acceptable readings as a function of the relative error δ (difference between a given measurement and the average of the 5 readings). The grayed out box illustrates a maximum acceptable error of $\delta = 20\%$, when the fraction of acceptable readings is 78%. The red line shows a logistic fit ($R^2 = 0.995$).

221 measuring methods [28, 41, 42], and has not been demonstrated by other studies. We are
 222 not aware of earlier studies that have successfully performed the CRT test in volunteers
 223 of all skin phototypes (Table 1).

224 For all volunteers studied, the G-channel average intensity presented an approx-
 225 imately exponential decay with good signal-to-noise ratio (SNR) compared to the other
 226 channels. While the R-channel exhibited negligible CRT signal for all phototypes (Fig-
 227 ure 2a is typical), The B channel displayed a clear pCRT signal for individuals with low
 228 melanin skin tones (Figure 2a, for example). However, for phototypes V-VI, the B chan-
 229 nel either showed no pCRT signal or had poor SNR due to increased melanin absorption.
 230 In contrast, the G-channel consistently enabled pCRT readings with a good SNR regard-
 231 less of the phototype. This can be attributed to a tradeoff between light absorption and
 232 scattering by the skin (which varies based on melanin levels) and light absorption by
 233 hemoglobin[43].

234 We developed a flagging recipe to discard-and-repeat most poor readings. Thus,
 235 the chance of an erroneous reading is reduced at the cost of increasing the fraction of
 236 rejected readings. On observing the data, we chose readings with relative regression
 237 uncertainty lower than of 10% to be “acceptable readings”. Notice that the regression
 238 uncertainty pertains only to the regression method and is not the same thing as an uncer-
 239 tainty or error in the pCRT reading. Out of the acceptable readings, 80% (CI 95%) had a
 240 relative error (δ) lower than $0.2\langle pCRT \rangle$ (Figure6b).

241 The combined variability due to physiology and measurement method gives a SD

242 = 30% without discarding readings, and SD = 17% when readings with relative regression
243 uncertainty higher than 10% are discarded (Figure 6a). Averaging two or more readings
244 can further decrease the fraction of readings with low relative error δ . In practice, a
245 compromise must be made among discarding and repeating readings, and risking a high
246 relative error result.

247 The use of an exponential regression with a cutoff time contributes to the repro-
248 ducibility of the pCRT results. After the end of the steep decay region of the curve, in
249 some individuals the curve becomes noisy and in other individuals the exponential time
250 constant may change (Figure 3, graphs below the images). We believe that these changes
251 are caused by mechanical changes in elasticity of the skin, and by different time dynamics
252 of subjacent fat and muscle, which also depend on the state of hydration of the tissue[44].
253 To stabilize the exponential regression, we established a cutoff time to limit the expo-
254 nential fit to the region of steep fall of the curve, as detailed in section 3.3. The cutoff
255 strategy improves the quality of the exponential regressions and the repeatability of the
256 readings. Except for the cutoff strategy, our regression method follows approximately the
257 one proposed by Shinozaki et al.[31] that calculates CRT fitting and exponential decay to
258 the grayscale video signal. They use a cutoff between 90% and 10% of the decay curve
259 and do not take advantage of regression uncertainties.

260 Though pCRT relates to the same physiological parameters as CRT and yields
261 values similar to the visual CRT measurement method [7, 45], they differ in values. The
262 values for pCRT are larger than for visual CRT. The difference may be due to the lower
263 pressure we apply (7 kPa) compared to conventional CRT [12, 31, 46, 47] and/or to the
264 improved visibility of blood perfusion in the skin provided by cocircular polarized imag-
265 ing. The compression applied to induce whitening of the ROI is one of the many factors
266 known to influence the CRT [27, 48]. Ordinarily, these compressions are subjective and
267 are typically applied with the examiner's fingertip. Different researchers have proposed
268 different compressions. For example, Kawaguchi et al. propose a pressure of 10 kPa - 70
269 kPa applied with the fingertip for 2 seconds as optimal [46]. Other studies have proposed
270 17 kPa [12, 47], and 60 kPa [31]. We have adopted throughout this study the lowest pres-
271 sure yet, 7 kPa, which is low enough not to induce any pain in the forearm. With this
272 low pressure, we demonstrated repeatability. In another study to be published elsewhere,
273 we noticed that application of high pressure in the forearm (23 kPa) increased noise, de-
274 creased fit quality, and repeatability. Our success with using low pressure (7 kPa) may
275 be attributed not only to the higher sensitivity of digital cameras but also to the use of
276 cocircular polarizers, which improves SNR by attenuating the component due to reflec-
277 tion on the skin surface [36, 39, 40]. We believe that with adequate image processing and
278 illumination aimed to avoid reflections, the polarizers may be unnecessary.

279 We chose to assess CRT on the forearm instead of the fingertip for two main
280 reasons. First, given the primary objective of our study, which focused on investigating the
281 robustness of the technique, we recognized that the fingertip, due to its high susceptibility
282 to peripheral temperature changes, could introduce additional variability into the results
283 [27, 24]. The forearm provides a more stable baseline for our measurements. Second,
284 by incorporating forearm assessments, we aimed to expand the existing body of literature
285 on CRT studies, thereby advancing the overall understanding and practical application of
286 this technique.

287 Limitations of this study include the utilization of data from a healthy group aged
288 20–70 years, thereby minimizing the confounding effects of disorders or diseases on
289 the obtained results. However, as demonstrated by several previous studies, it is well-
290 established that depending on the specific disease, pCRT values would deviate from the
291 values found in a healthy control group [23, 33, 22, 49]. Another potential limitation
292 involves the potential interference of the cardiovascular and parasympathetic systems in
293 the volunteers during the five CRT readings. Volunteers may have found the experiment
294 to be stressful or at least initially uncomfortable due in part to the cold, unlit environ-
295 ment, unfamiliar equipment, and the requirement to stay still during most of the process.
296 This situation may have caused the activation of the sympathetic nervous system of some
297 volunteers during data acquisition, which induces a change in the heart rate (HR) [1, 50].
298 Heart rate and temperature are factors known to influence CRT [51], this may have caused
299 intra-participant pCRT variation along the 5 readings. Other limitations of this study are
300 the lack of skin temperature measurement, and the relatively small number of volunteers
301 did not allow further investigations on pCRT dependence with multiple variables.

302 The robustness of different phototypes and a good repeatability of pCRT opens up
303 the possibility for health condition status tracking and physiological monitoring studies
304 where the conventional CRT method has proved unreliable. Among possibilities that
305 remain to be studied are the relationship between pCRT and temperature, heart rate, blood
306 pressure, or with the autonomic nervous system.

307 **6. Conclusion**

308 We have demonstrated that CRT can be made robust, independent of the observer and skin
309 color, and can be performed at low compression using simple equipment. These findings
310 hold promise for further research in a clinical setting and quantitative CRT. Further ad-
311 vancements of the method have the potential to reliably assess an individual’s capillary
312 refill time over time, facilitating effective tracking of health conditions.

313 **7. Acknowledgements**

314 The authors thank Beatriz Janke and Carlos Renato da Silva, for experimental help, and
315 all the volunteers who participated in the experiment.

316 **8. Supplementary Materials**

317 The code used for this work is available at [https://github.com/Photobiomedical-
318 Instrumentation-Group/pCRTMatlab](https://github.com/Photobiomedical-Instrumentation-Group/pCRTMatlab)

319 **9. Author Contributions**

320 Conceptualization R.P.d.S.B., E.L.D, and G.C.C.; Formal analysis, R.P.d.S.B., E.L.D, and
321 G.C.C; Methodology, R.P.d.S.B.; Software, R.P.d.S.B.; Supervision, G.C.C.; Validation,
322 G.C.C.; Writing—original draft, R.P.d.S.B.; Writing—review and editing, R.P.d.S.B.,
323 E.L.D, and G.C.C. All authors contributed to the article and approved the submitted ver-
324 sion.

325 **10. Funding**

326 This study was financed by the Coordenação de Aperfeiçoamento de Pessoal de Nível
327 Superior—Brazil (CAPES)—Finance Code 001.

328 **11. Informed Consent Statement**

329 Informed consent was obtained from all subjects involved in the study.

330 **12. Conflict of interest**

331 The authors declare no conflicts of interest.

332 **References**

- [31] David L. Schriger and Larry Baraff. Defining normal capillary refill: Variation with age, sex, and temperature. *Annals of Emergency Medicine*, 17(9):932–935, 1988.
- [32] D. A. Osborn, N. Evans, and M. Kluckow. Clinical detection of low upper body blood flow in very premature infants using blood pressure, capillary refill time, and central-peripheral temperature difference. *Archives of Disease in Childhood: Fetal and Neonatal Edition*, 89(2), 2004.
- [33] Alexandre Lima, Tim C Jansen, Jasper Van Bommel, Can Ince, and Jan Bakker. The prognostic value of the subjective assessment of peripheral perfusion in critically ill patients. *Critical Care Medicine*, 37(3):934–938, mar 2009.
- [44] Emilio Daniel Valenzuela Espinoza, Sebastián Welsh, and Arnaldo Dubin. Lack of agreement between different observers and methods in the measurement of capillary refill time in healthy volunteers: An observational study. *Revista Brasileira de Terapia Intensiva*, 2014.
- [45] David King, Robert Morton, and Cliff Bevan. How to use capillary refill time. *Archives of Disease in Childhood: Education and Practice Edition*, 2014.
- [46] A Nickel, S Jiang, N Napolitano, K Saeki, and H Hirahara Circulation. Impact of Skin Color on Accuracy of Capillary Refill Time Measurement by Pulse Oximeter. *Am Heart Assoc*, 2018.
- [47] Amelia Pickard, Walter Karlen, and J. Mark Ansermino. Capillary refill time: Is it still a useful clinical sign? *Anesthesia and Analgesia*, 113(1):120–123, 2011.
- [48] ADAM Watson and Anne-Maree Kelly. Measuring capillary refill time is useless. *Emergency Medicine*, 5(2):90–93, jun 1993.
- [49] N. Venkata Raju, M. Jeffrey Maisels, Elizabeth Kring, and Laura Schwarz-Warner. Capillary refill time in the hands and feet of normal newborn infants. *Clinical Pediatrics*, 38(3):139–144, 1999.
- [10] Elizabeth Bridges. Assessing Patients during Septic Shock Resuscitation. *American Journal of Nursing*, 117(10):34–40, 2017.
- [16b] Jodie Crook and Rachel M Taylor. The agreement of fingertip and sternum capillary refill time in children. *Archives of Disease in Childhood*, 98(4):265–268, 2013.
- [12] L. L. Blaxter, D. E. Morris, J. A. Crowe, C. Henry, S. Hill, D. Sharkey, H. Vyas, and B. R. Hayes-Gill. An automated quasi-continuous capillary refill timing device. *Physiological Measurement*, 37(1):83–99, dec 2015.
- [13] MH Gorelick, KN Shaw, MD Baker Pediatrics, and Undefined 1993. Effect of ambient temperature on capillary refill in healthy children. *Am Acad Pediatrics*, 1993.

- [14] Hattan K. Ballaji, Ricardo Correia, Chong Liu, Serhiy Korposh, Barrie R. Hayes-Gill, Alison Musgrove, and Stephen P. Morgan. Optical fibre sensor for capillary refill time and contact pressure measurements under the foot. *Sensors*, 21(18):6072, sep 2021.
- [15] Monija Mrgan, Dorte Rytter, and Mikkel Brabrand. Capillary refill time is a predictor of short-term mortality for adult patients admitted to a medical department: An observational cohort study. *Emergency Medicine Journal*, 31(12):954–958, dec 2014.
- [16] Yuwarat Monteerarat, Roongsak Limthongthang, Panai Laohaprasitiporn, and Torpon Vathana. Reliability of capillary refill time for evaluation of tissue perfusion in simulated vascular occluded limbs. *European Journal of Trauma and Emergency Surgery*, pages 1–7, jan 2021.
- [17] Abhishek Pandey and BM John. Capillary refill time. is it time to fill the gaps? *Medical Journal, Armed Forces India*, 69(1):97, 2013.
- [18] H. Ait-Oufella, N. Bige, P. Y. Boelle, C. Pichereau, M. Alves, R. Bertinchamp, J. L. Baudel, A. Galbois, E. Maury, and B. Guidet. Capillary refill time exploration during septic shock. *Intensive Care Medicine*, 40(7):958–964, 2014.
- [19] H. Otieno, E. Were, I. Ahmed, E. Charo, A. Brent, and K. Maitland. Are bedside features of shock reproducible between different observers? *Archives of Disease in Childhood*, 89(10):977–979, oct 2004.
- [20] Itai Shavit, Rollin Brant, Cheri Nijssen-Jordan, Roger Galbraith, and David W. Johnson. A novel imaging technique to measure capillary-refill time: Improving diagnostic accuracy for dehydration in young children with gastroenteritis. *Pediatrics*, 118(6):2402–2408, dec 2006.
- [21] Susannah Fleming, Peter Gill, Caroline Jones, James A. Taylor, Ann Van Den Bruel, Carl Heneghan, Nia Roberts, and Matthew Thompson. The diagnostic value of capillary refill time for detecting serious illness in children: A systematic review and meta-analysis. *PLoS ONE*, 10(9), sep 2015.
- [22] World Health Organization. *Dengue: guidelines for diagnosis, treatment, prevention, and control*. World Health Organization, 2009.
- [23] Burcu Yormaz, Hilay Akay Cizmecioglu, Mevlut Hakan Goktepe, Nijat Ahmadli, Dilek Ergun, Baykal Tulek, Fikret Kanat, and Ahmet Cizmecioglu. Is Capillary Refill Time an Early Prognostic Factor in COVID-19 Patients. *Selcuk Tip Dergisi*, 3(37):224–230, 2021.
- [24] Koichiro Shinozaki, Lee S Jacobson, Kota Saeki, Naoki Kobayashi, Steve Weisner, Julianne M Falotico, Timmy Li, Junhwan Kim, Joshua W Lampe, and Lance B Becker. Does training level affect the accuracy of visual assessment of capillary refill time? *Critical care (London, England)*, 23(1):157, 2019.
- [25] Bronwyn Anderson, Anne Maree Kelly, Debra Kerr, and Damien Jolley. Capillary refill time in adults has poor inter-observer agreement. *Hong Kong Journal of Emergency Medicine*, 15(2):71–74, apr 2008.

- [26] Lawrence H. Brown, N. Heramba Prasad, and Theodore W. Whitley. Adverse lighting condition effects on the assessment of capillary refill. *American Journal of Emergency Medicine*, 12(1):46–47, 1994.
- [27] Rani Toll John, Joakim Henricson, Johan Junker, Carl Oscar Jonson, Gert E. Nilsson, Daniel Wilhelms, and Chris D. Anderson. A cool response—The influence of ambient temperature on capillary refill time. *Journal of Biophotonics*, 11(6):e201700371, jun 2018.
- [28] A. Matas, M. G. Sowa, V. Taylor, G. Taylor, B. J. Schattka, and H. H. Mantsch. Eliminating the issue of skin color in assessment of the blanch response. *Advances in skin & wound care*, 14(4):180–188, 2001.
- [29] J. Lewin and I. Maconochie. Capillary refill time in adults. *Emergency Medicine Journal*, 25(6):325–326, jun 2008.
- [30] Todd P. Chang, Genevieve Santillanes, Ilene Claudius, Phung K. Pham, James Koved, John Cheyne, Marianne Gausche-Hill, Amy H. Kaji, Saranya Srinivasan, J. Joelle Donofrio, and Cynthia Bir. Use of a Novel, Portable, LED-Based Capillary Refill Time Simulator within a Disaster Triage Context. *Prehospital and Disaster Medicine*, 2017.
- [31] Koichiro Shinozaki, Lee S. Jacobson, Kota Saeki, Hideaki Hirahara, Naoki Kobayashi, Steve Weisner, Julianne M. Falotico, Timmy Li, Junhwan Kim, and Lance B. Becker. Comparison of point-of-care peripheral perfusion assessment using pulse oximetry sensor with manual capillary refill time: Clinical pilot study in the emergency department. *Journal of Intensive Care*, 7(1), nov 2019.
- [32] Emmett Kerr, Sonya Coleman, T. M. McGinnity, and Andrea Shepherd. Measurement of capillary refill time (CRT) in healthy subjects using a robotic hand. In *IEEE Computer Society Conference on Computer Vision and Pattern Recognition Workshops*, volume 2018-June, pages 1372–1379, 2018.
- [33] Ahmet Cizmecioglu, Dilek Tezcan, Selda Hakbilen, and Sema Yilmaz. Prolonged capillary refill time highlights early performing of nailfold capillaroscopy in patients with systemic sclerosis. *Konuralp Medical Journal*, 14(1):114–123, 2022.
- [34] Rani Toll John, Joakim Henricson, Chris D Anderson, and Daniel Björk Wilhelms. Man versus machine: Comparison of naked-eye estimation and quantified capillary refill. *Emergency Medicine Journal*, 36(8):465–471, aug 2019.
- [35] Steven L. Jacques, Jessica C. Ramella-Roman, and Ken Lee. Imaging skin pathology with polarized light. *Journal of Biomedical Optics*, 7(3):329, jul 2002.
- [36] Warren Groner, James W. Winkelman, Anthony G. Harris, Gerrit J. Bouma, Konrad Messmer, Richard G. Nadeau, Can Ince, Gerrit J. Bouma, Konrad Messmer, and Richard G. Nadeau. Orthogonal polarization spectral imaging: A new method for study of the microcirculation. *Nature Medicine*, 5(10):1209–1212, oct 1999.
- [37] I Stockford and S Morgan. Surface-reflection elimination in polarization imaging of superficial tissue. *Opt Lett*, 28(2), 2003.

- [38] Bronwyn Anderson, Anne Maree Kelly, Debra Kerr, Megan Clooney, and Damien Jolley. Impact of patient and environmental factors on capillary refill time in adults. *American Journal of Emergency Medicine*, 26(1):62–65, jan 2008.
- [39] I Stockford and S Morgan. Surface-reflection elimination in polarization imaging of superficial tissue. *Opt Lett*, 28(2):114–116, jan 2003.
- [40] Mariia Borovkova, Alexander Bykov, Alexey Popov, and Igor Meglinski. Influence of scattering and birefringence on the phase shift between electric field components of polarized light propagated through biological tissues. In Arjen Amelink and Seemantini K. Nadkarni, editors, *Optics InfoBase Conference Papers*, volume Part F142-, page 25. SPIE, jul 2019.
- [41] Jose M. Saavedra, Glenn D. Harris, Song Li, and Laurence Finberg. Capillary Refilling (Skin Turgor) in the Assessment of Dehydration. *American Journal of Diseases of Children*, 145(3):296–298, 1991.
- [42] Philip E. Bickler, John R. Feiner, and John W. Severinghaus. Effects of skin pigmentation on pulse oximeter accuracy at low saturation. *Anesthesiology*, 102(4):715–719, 2005.
- [43] Characterizing reduced scattering coefficient of normal human skin across different anatomic locations and Fitzpatrick skin types using spatial frequency domain imaging. *Journal of Biomedical Optics*, 26(02), feb 2021.
- [44] Alexey P. Popov, Alexander V. Bykov, and Igor V. Meglinski. Influence of probe pressure on diffuse reflectance spectra of human skin measured in vivo. *Journal of Biomedical Optics*, 22(11):1, nov 2017.
- [45] H. R. Champion, W. J. Sacco, D. S. Hannan, R. L. Lepper, E. S. Atzinger, W. S. Copes, and R. H. Prall. Assessment of injury severity: the triage index. *Critical care medicine*, 8(4):201–208, 1980.
- [46] Rui Kawaguchi, Taka-aki Nakada, Taku Oshima, Masayoshi Shinozaki, Toshiya Nakaguchi, Hideaki Haneishi, and Shigeto Oda. Optimal pressing strength and time for capillary refilling time. *Critical Care*, 23(1):1–3, 2019.
- [47] Chong Liu, Ricardo Correia, Hattan Ballaji, Serhiy Korposh, Barrie Hayes-gill, and Stephen Morgan. Optical fibre sensor for simultaneous measurement of capillary refill time and contact pressure. *Sensors (Switzerland)*, 20(5), 2020.
- [48] Valery V Tuchin, Dan Zhu, and Elina A Genina. *Handbook of Tissue Optical Clearing: New Prospects in Optical Imaging*. CRC Press, 2022.
- [49] Oi Yasufumi, Naoto Morimura, Aya Shirasawa, Hiroshi Honzawa, Yutaro Oyama, Shoko Niida, Takeru Abe, Shouhei Imaki, and Ichiro Takeuchi. Quantitative capillary refill time predicts sepsis in patients with suspected infection in the emergency department: An observational study. *Journal of Intensive Care*, 7(1):29, may 2019.
- [50] Youngjun Cho, Simon J. Julier, and Nadia Bianchi-Berthouze. Instant stress: Detection of perceived mental stress through smartphone photoplethysmography and thermal imaging. *Journal of Medical Internet Research*, 21(4), apr 2019.
- [51] Matthias Jacquet-Lagrèze, Nouredine Bouhamri, Philippe Portran, Rémi Schweizer, Florent Baudin, Marc Lilot, William Fornier, and Jean-Luc Fellahi. Capillary refill time

489 variation induced by passive leg raising predicts capillary refill time response to vol-
490 ume expansion. *Critical Care*, 23(1):281, dec 2019.